

Rotational bands in odd-odd ^{182}Re

M. F. Slaughter,* R. A. Warner,[†] T. L. Khoo,[‡] W. H. Kelly,[§] and Wm. C. McHarris
*National Superconducting Cyclotron Laboratory and Departments of Physics and Astronomy and of Chemistry,
 Michigan State University, East Lansing, Michigan 48824*

(Received 25 May 1983)

Rotational bands in the odd-odd nucleus, ^{182}Re , have been studied via the $^{181}\text{Ta}(\alpha, 3n\gamma)^{182}\text{Re}$, $^{182}\text{W}(p, n\gamma)^{182}\text{Re}$, and $^{184}\text{W}(p, 3n\gamma)^{182}\text{Re}$ reactions, using Ge γ -ray detectors in a variety of singles, coincidence, delayed coincidence, and angular distribution experiments. Four rotational bands were characterized extensively: $7^+\{\pi_{\frac{5}{2}}^+[402\uparrow]\otimes\nu_{\frac{9}{2}}^+[624\uparrow]\}$, triplet coupling (64-h $^{182}\text{Re}^g$) to $J=16$; 2^+ , singlet coupling (12.7-h $^{182}\text{Re}^m$), to $J=12$; $9^-\{\pi_{\frac{9}{2}}^-[514\uparrow]\otimes\nu_{\frac{9}{2}}^+[624\uparrow]\}$, triplet band head ($t_{1/2}=6\pm 2$ ns) at 443.1 keV, to $J=15$; and $4^-\{\pi_{\frac{1}{2}}^-[541\uparrow]\otimes\nu_{\frac{9}{2}}^+[624\uparrow]\}$, triplet band head ($t_{1/2}=780\pm 90$ ns) at 461.3 keV above $^{182}\text{Re}^m$. All four bands are highly distorted from Coriolis effects. g_K and g_R were deduced and agree with the assigned configurations. A four-quasiparticle isomer ($t_{1/2}=88\pm 8$ ns) was located at 2256.3 keV and is characterized as an oblate girdle about the basic prolate core.

<p>NUCLEAR REACTIONS $^{181}\text{Ta}(\alpha, 3n\gamma)^{182}\text{Re}$, $^{182}\text{W}(p, n\gamma)^{182}\text{Re}$, $^{184}\text{W}(p, 3n\gamma)^{182}\text{Re}$; γ-ray singles, γ-γ coin, delayed coin, γ-θ; Ge detectors; determined E_γ, I_γ, $I_\gamma(\theta)$, g_K, g_R; deduced states in odd-odd ^{182}Re, J^π, K, $t_{1/2}$; calculated rotational band parameters, Coriolis effects, isomer configuration.</p>

I. INTRODUCTION

In odd-odd nuclei nature has provided us with microcosmic laboratories for studying the proton-neutron residual interactions. However, there are some serious complications and strings attached. Low Q values for β decay from their even-even parents prevent comprehensive studies except for nuclei quite far from stability, and only in recent years have experimental and computational techniques been developed to deal handily with nuclei far from stability. Also, the very high level density of odd-odd nuclei has made their study by in-beam spectroscopy difficult. Even when relatively complete level schemes have been worked out by high-resolution in-beam γ -ray spectroscopy, for example, the abundance of states and consequent ease of configuration interaction and mixing has made interpretation of the states rather tenuous. The result, of course, is that published studies and analyses of odd-odd nuclei are few and far between. Nature's micro-labs have had few tenants.

Highly deformed odd-odd nuclei are perhaps the most accessible, both to experiment and to interpretation. Here the difficulties are ameliorated in three ways: First, the fact that states come in bands rather than singly gives one a powerful handle with which to sort them out. Second, because of projection quantum numbers, these nuclei have only algebraic, rather than vectorial, couplings between the odd-proton and odd-neutron states. Although the overall density of states remains very high, the number of *intrinsic* states below a given excitation energy is considerably lower than in comparable odd-odd spherical nuclei. Last, and by no means least, because of the enhanced nature of intraband γ transitions, there is a tendency for a

highly excited nucleus to "lock in" on one or a few rotational bands and to deexcite primarily by these. This is particularly true when intrinsic high-spin bands are available that can provide yrast or near-yrast states up to or near the entrance population of states excited by the reaction that formed the nucleus in question.

$^{182}_{75}\text{Re}_{107}$ thus makes a good odd-odd candidate for study. It lies in a well-deformed region, targets are readily available for its production for in-beam γ -ray spectroscopic studies, and both single-particle and collective modes of excitation have been reasonably well characterized in many nearby nuclei.

Prior to this work the following was known about ^{182}Re :

Some dozen or so low-lying, low-spin states in ^{182}Re had been identified through the electron-capture decay of 22.0-h ^{182}Os .¹⁻⁷ Both because of the $J^\pi=0^+$ of ^{182}Os and its small decay energy ($Q_\epsilon \approx 850$ keV), an insufficient number of states was excited in any one band to enable much to be done in the way of organizing the states into bands or of characterizing any bands themselves. Assignments of structures were made pretty much on the basis of expected systematics and reasonable self-consistency. (There is a considerable amount of disagreement among the findings in Refs. 1-7.)

Two isomers of ^{182}Re itself are known,⁸ a $J^\pi=7^+$ 64-h activity and a 2^+ 12.7-h activity, the latter presumably the "ground state" populated by ^{182}Os decay. The decay schemes of these have been studied in detail, and they populate high-spin⁸⁻¹¹ and low-spin^{10,12-14} states, respectively, in ^{182}W . There is no observable isomeric transition between the two isomers, and the 7^+ 64-h isomer decays exclusively by electron capture to higher-lying states in

^{182}W , so the energy relationship between the two has not been determined experimentally. It was suggested¹⁵ that the two are the triplet ($\Sigma=1$) and singlet ($\Sigma=0$) couplings of the $\pi_{\frac{5}{2}^+}[402\uparrow]$ and $\nu_{\frac{9}{2}^+}[624\uparrow]$ Nilsson single-particle states, and this is corroborated by recent determinations⁸ of their magnetic moments. Assuming the validity of the Gallagher-Moszkowski coupling rules,¹⁶ this means that the (triplet) 7^+ 64-h isomer is $^{182}\text{Re}^g$ and the (singlet) 2^+ 12.7-h isomer is $^{182}\text{Re}^m$. The energy difference between them is expected to be of the order of (many) tens of keV.

In-beam γ -ray studies on ^{182}Re were first performed by Hjorth, Ryde, and Skånberg,¹⁷ who by means of γ -ray singles and angular distribution data [taken with a Ge(Li) detector] from the $^{181}\text{Ta}(\alpha,3n\gamma)^{182}\text{Re}$ reaction identified two rotational bands, each of six members. They suggested $K=7$ for the “lower” band and $K=4$ or 5 for the “upper” one.

The position of these bands was reversed by Medsker *et al.*,¹⁸ who also used the $^{181}\text{Ta}(\alpha,3n\gamma)^{182}\text{Re}$ reaction but added γ - γ coincidence measurements. They suggested a

$$7^+ \{ \pi_{\frac{5}{2}^+}[402\uparrow] \otimes \nu_{\frac{9}{2}^+}[624\uparrow] \}$$

assignment for the lower band and a

$$9^- \{ \pi_{\frac{9}{2}^-}[514\uparrow] \otimes \nu_{\frac{9}{2}^+}[624\uparrow] \}$$

assignment for the upper one.

We have studied rotational bands in ^{182}Re populated via the $^{181}\text{Ta}(\alpha,3n\gamma)^{182}\text{Re}$ reaction, supplemented by the $^{182}\text{W}(p,n\gamma)^{182}\text{Re}$ and $^{184}\text{W}(p,3n\gamma)^{182}\text{Re}$ reactions. Using various combinations of Ge(Li) detectors we have performed γ -ray singles, coincidence (γ - γ - t), and angular-distribution experiments. Our results confirm the band placements and assignments of Medsker *et al.* and extend the bands up to high-spin members. We have identified two new bands with $K=2^+$ and 4^- and a high-spin ($J \geq 15$) metastable ($t_{1/2} = 88 \pm 8$ ns) state at 2256.4 keV. Also, from branching ratios obtained for the 7^+ band, together with the recently measured g factor of $^{182}\text{Re}^g$, we infer the value of g_R to be 0.10 ± 0.07 . We discuss the bands in terms of Nilsson state assignments and extract band parameters, including the effects of Coriolis coupling. No backbending was observed for any of the bands. [Since only moderate values of the rotational angular momentum ($\bar{R} \lesssim 10$) were attained, this is not a stringent test of the rotationally aligned pair model of backbending, where backbending would be expected only at higher values of \bar{R} , if at all.] Finally, the high-spin metastable state is discussed as a possible candidate for a “near-yrast trap,” i.e., four-quasiparticle state with the \vec{j} ’s aligned mostly *along* the axis of *symmetry* thereby producing an “oblate girdle” about the basic prolate core and a possible “band head” for an *effective* rotation about the axis of symmetry, similar to those observed in even-even Hf isotopes.

II. EXPERIMENTAL

A. Target and $(\alpha,3n\gamma)$ reaction

A self-supporting, ≈ 4 mg/cm² thick foil of natural Ta (99.988% ^{181}Ta) was the target for the $^{181}\text{Ta}(\alpha,3n\gamma)^{182}\text{Re}$ reaction. The α -particle beam from the Michigan State University 50-MeV sector-focused cyclotron was used, and a rough excitation function established that the optimum α -particle energy for the $^{181}\text{Ta}(\alpha,3n\gamma)^{182}\text{Re}$ reaction was 38 MeV.

B. Singles γ -ray spectra

Singles γ -ray spectra were taken with a low-energy photon spectrometer (LEPS), a Ge(Li) detector having a resolution of 650 eV for the ^{57}Co 122-keV line. This detector was oriented at 125° relative to the beam direction in order to minimize effects due to angular distributions of the γ rays— 125° is a node of P_2 . Data were recorded for γ rays up to 1 MeV in energy, and the spectra were analyzed in the standard manner, using the computer code SAMPO.¹⁹ A resulting singles spectrum is shown in Fig. 1. The 61 γ rays we identified as originating from ^{182}Re are listed in Table I, together with the intensities we determined from these data. Unless otherwise noted, only γ rays seen in coincidence with assigned transitions (cf. below) are included.

C. γ - γ - t coincidence spectra

Three parameter γ - γ - t coincidence data were taken using two true-coaxial Ge(Li) detectors having 4.5% and 7% efficiencies and ≈ 2.1 keV resolutions FWHM for the ^{60}Co 1333-keV γ ray. These detectors were placed at $\pm 90^\circ$ to the beam direction, and absorbers of about 0.3 cm each of Cu and Cd foil were placed in front of the detectors to minimize the contributions of x rays to the count rate. The data were written event by event on magnetic tape for later off-line sorting and analysis; a resolving time 2τ of ≈ 60 ns was used. Some 27×10^6 events were accumulated during the two-day experiment. An integral coincidence

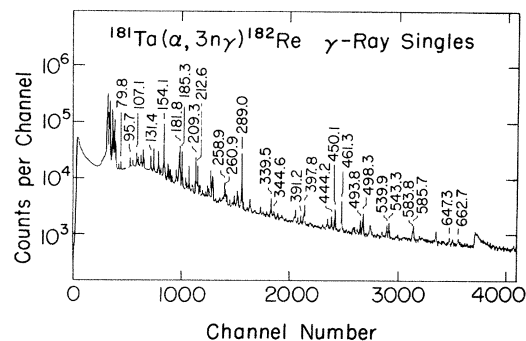


FIG. 1. Singles γ -ray spectrum from the $^{181}\text{Ta}(\alpha,3n\gamma)^{182}\text{Re}$ reaction taken with a LEPS Ge(Li) detector. Only the more intense γ rays are labeled in this figure; for a complete listing, see Table I.

TABLE I. γ -rays observed from the $^{181}\text{Ta}(\alpha,3n\gamma)^{182}\text{Re}$ reaction.

E_γ (keV) ^a	I_γ	E_γ (keV) ^a	I_γ
55.6 ^b	b	268.0	3.2(0.2)
76.3	2.4(0.2)	276.0 ^d	6.1(0.4)
79.8	3.4(0.2)	281.2(0.2)	11(1)
95.7	4.2(0.3)	282.3(0.2)	6(1)
107.1 ^c	7.9(0.5)	289.0	≡ 100
119.5	5.3(0.3)	292.2	4.4(0.3)
131.4	8.8(0.2)	303.0	6(1)
136.4 ^d	17(1)	303.6	4(1)
152.3(0.2)	1.6(0.4)	321.3	4.2(0.3)
154.1	80(5)	323.3	2.5(0.2)
160.4(0.2)	11.7(0.7)	339.5 ^{c,d}	14(1)
161.3(0.2)		341.7	1.8(0.2)
175.1 ^d	8(1)	344.6	3.4(0.3)
179.3	8(1)	358.2(0.2)	1.5(0.2)
180.2	31(2)	391.2	5.1(0.3)
181.8	43(3)	395.9	6.4(0.4)
185.3	36(2)	397.8	17(1)
191.6 ^d	6.3(0.4)	437.6	6.5(0.4)
197.2 ^d	18(1)	444.2	9.2(0.6)
209.3	37(2)	450.1	18(1)
210.6	5.5(0.3)	461.3	33(2)
212.6	23(2)	493.8	11(1)
217.0	4.3(0.5)	498.3 ^c	21(1)
220.8	2.5(0.3)	539.9	8.4(0.5)
230.1(0.3) ^d		543.3	13(1)
231.8	5.5(0.3)	583.8	6.9(0.5)
234.9	23(1)	585.7	13(0.8)
237.6	16(1)	624.5	9(1)
258.9	15(1)	647.3	4.9(0.4)
260.9	8.9(0.5)	662.7	3.6(0.3)
263.3	6.3(0.4)		

^aUnless otherwise indicated, the uncertainty in E_γ is ± 0.1 keV.

^bBecause of the low-energy background, we could not see this γ ray; however, it has been observed and placed from ^{182}Os decay (Ref. 1).

^cThis peak is an unresolved multiplet of ^{182}Re γ rays.

^dThis peak is an unresolved multiplet containing a component from a nucleus produced by competing reactions.

spectrum is shown in Fig. 2, and illustrative gated spectra are shown in Fig. 3. Following the coincidence experiment, the LEPS detector was used to count the residual target activity. Approximately 90% of this activity resulted from 64-h ^{182}Re .

D. Delayed spectra

Early in our coincidence experiments it became evident that a number of states in ^{182}Re had half-lives commensurate or long in comparison with the resolving time. Thus, we investigated the delayed spectra resulting from the deexcitation of these states with the LEPS detector and a beam sweeper on the cyclotron. The beam sweeper deflects a variable fraction of the cyclotron beam bursts away from the target. Spectra (both singles and coincidence) were taken during the interval the beam was off, with this interval being divided into nine equal time

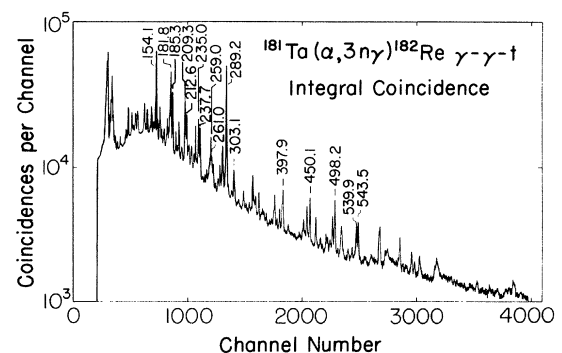


FIG. 2. Integral coincidence spectrum from the $^{181}\text{Ta}(\alpha,3n\gamma)^{182}\text{Re}$ reaction.

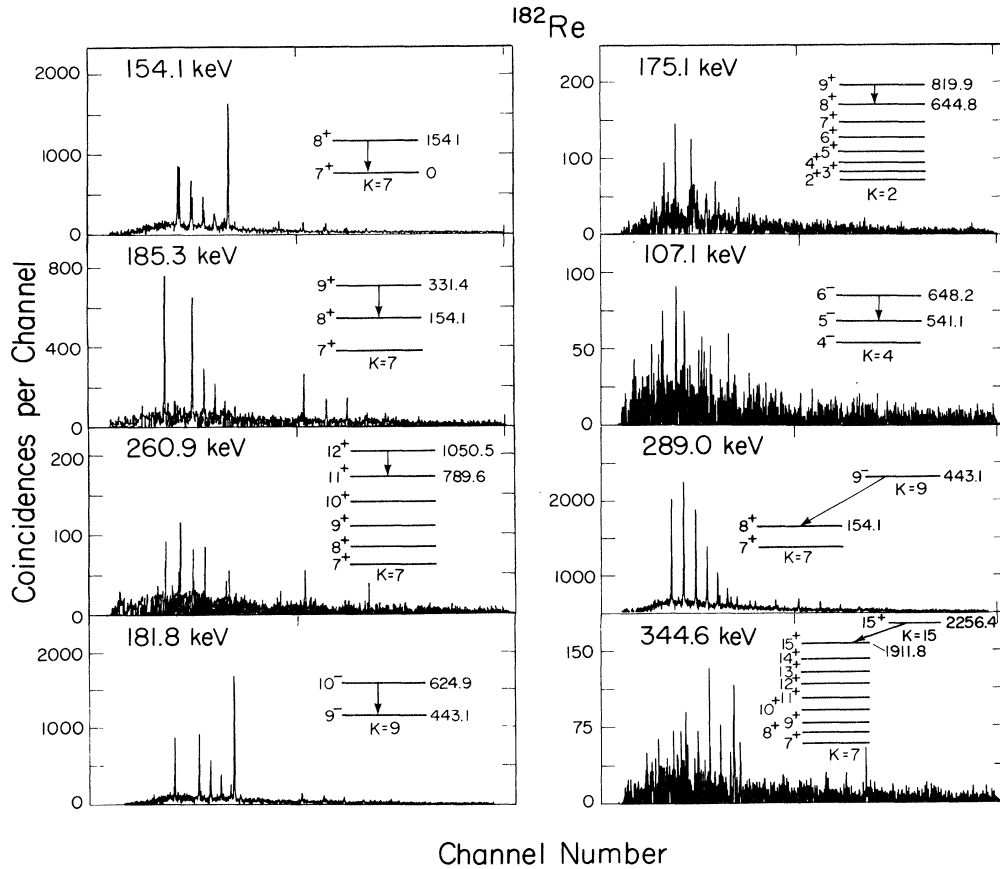


FIG. 3. Selected gates coincidence spectra from the $^{181}\text{Ta}(\alpha,3n\gamma)^{182}\text{Re}$ reaction. These are gated slices of the spectrum shown in Fig. 2. They illustrate gates set on transitions within each of the four major rotational bands observed in ^{182}Re and also on two of the important interband transitions.

bands. Two time ranges were investigated. The shorter one used intervals between beam bursts, with an overall time scale of ≈ 50 ns. The longer one had the beam deflected away from the target for eight bursts or ≈ 400 ns. These experiments will be referred to in more detail at the appropriate places while discussing construction of the level scheme.

E. γ -ray angular distributions

We used the LEPS detector in a goniometer to obtain γ -ray angular distributions. Data were collected at six angles (taken in random order) relative to the beam direction: 90° , 105° , 115° , 130° , 140° , and 145° . (Data taken for the last angle, 105° , were of poorer quality because of the buildup of ^{182}Re activity in the target, so they were generally omitted from the analysis.) The γ -ray peak areas were evaluated and fitted to the usual expression,

$$W(\theta) = A_0 + A_2 P_2(\cos\theta) + A_4 P_4(\cos\theta).$$

In Fig. 4 we show some examples of least-squares fits to the data. A_2/A_0 and A_4/A_0 coefficients derived from the fits are listed in Table II. Target and product x rays were used for the normalizations.

F. $(p,n\gamma)$ and $(p,3n\gamma)$ reactions

Two new rotational bands of low K were identified in our $(\alpha,3n\gamma)$ experiments. Since the $(\alpha,3n\gamma)$ reaction preferentially excites states of higher spin, we performed $(p,n\gamma)$ and $(p,3n\gamma)$ experiments, hoping to gain further information on these low- K bands. We used a 10-MeV beam of protons from the MSU 50-MeV sector-focused cyclotron on a ^{182}W target to induce the $^{182}\text{W}(p,n\gamma)^{182}\text{Re}$ reaction and a 29-MeV beam on a ^{184}W target to induce the $^{184}\text{W}(p,3n\gamma)^{182}\text{Re}$ reaction. The targets were enriched to $\approx 95\%$ in their respective isotopes (obtained from Oak Ridge National Laboratory) and were mounted on Formvar. A singles γ -ray spectrum, taken by the LEPS detector, from the $^{182}\text{W}(p,n\gamma)^{182}\text{Re}$ reaction is shown in Fig. 5. These proton-induced reactions did not produce significant new information regarding the previously identified bands.

III. LEVEL SCHEME

The ^{182}Re level scheme we were able to construct from our in-beam γ -ray data is shown in Fig. 6. For comparison, the (low-spin) states populated by the decay^{1,2} of ^{182}Os are shown in Fig. 7.

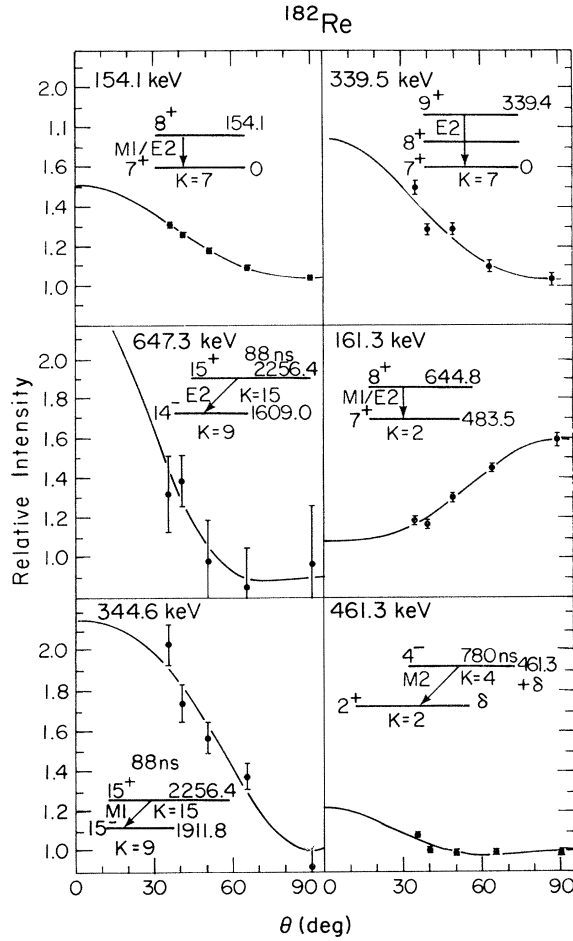


FIG. 4. Angular distributions for selected γ rays, showing different multiplicities, from the $^{181}\text{Ta}(\alpha,3n\gamma)^{182}\text{Re}$ reaction. The curves are least-square fits to the data points.

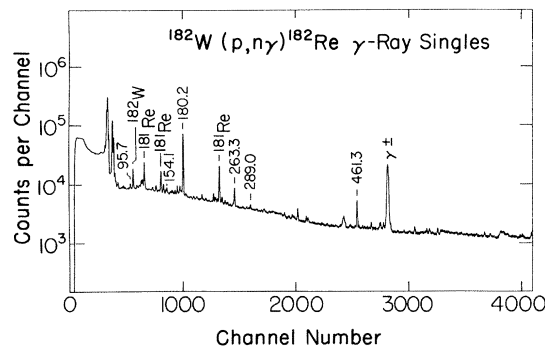


FIG. 5. Singles γ -ray spectrum from the $^{182}\text{W}(p,n\gamma)^{182}\text{Re}$ reaction taken with a LEPS Ge(Li) detector. Only a few intense γ rays are labeled for orientation purposes.

A. 7^+ and 9^- bands

States in odd-odd nuclei can be characterized by coupling the known single-particle states found in their odd-mass neighbors. Figure 8 shows the positions of these odd-mass states: the $A=181$ states were taken from the compilation of Ref. 20; the $A=183$ states, from Ref. 21. We would thus expect the ground state of ^{182}Re to result from coupling the $\frac{5}{2}^+[402\uparrow]$ proton state with the $\frac{9}{2}^+[624\uparrow]$ neutron state. This coupling produces a 7^+ triplet ($\Sigma=1$) state and a 2^+ singlet ($\Sigma=0$) state, and, according to the Gallagher-Moszkowski coupling rules,¹⁶ the triplet state should lie some tens of keV lower. Presumably, then, the 7^+ coupling is the ground state, while the 2^+ coupling could well be the metastable state. Atomic beams experiments²² have in fact established that 12.7-h ^{182}Re has a spin of 2, and the decay¹¹ of 64-h ^{182}Re has narrowed its assignment to $7^+, 6^\pm$. The two known isomers of ^{182}Re are thus consistent with the predicted coupling, with the 7^+ 64-h isomer being $^{182}\text{Re}^g$, the 2^+ 12.7-h isomer being $^{182}\text{Re}^m$. Because of the large spin difference, no isomeric transitions between the two can be observed. (The Moszkowski single-particle estimate²³ for a 100-keV $M5$ transition yields a half-life of $\approx 10^8$ yr, and even correcting this for a conversion coefficient of $\approx 10^3$ leaves little hope of ever observing such a transition.) For the purposes of this work we shall assume the 7^+ state to be $^{182}\text{Re}^g$. Numerous coincidence relations among the γ rays allow us to construct a rotational band on this 7^+ state, definitely up to the 14^+ member and very likely as high as the 16^+ member. We shall see (in Sec. V below) that the band parameters corroborate this assignment.

Our assignment of

$$7^+ \{ \pi \frac{5}{2}^+[402\uparrow] \otimes \nu \frac{9}{2}^+[624\uparrow] \}$$

for this lowest band in ^{182}Re is consistent with that of Medsker *et al.*,¹⁸ who reversed the positions of the bands originally suggested by Hjorth, Ryde, and Skånberg.¹⁷ The K values originally assigned by Hjorth, Ryde, and Skånberg were too small because they did not include Coriolis coupling. (The Coriolis operator²⁴ introduces a negative $J(J+1)$ term and a positive $J^2(J+1)^2$ term into the rotational-energy expansion. This means that the apparent value of K obtained from a straightforward application of the rotational-energy equation is too small unless these terms are taken into account. The $\nu \frac{9}{2}^+[624\uparrow]$ state, which enters into both of the bands they originally observed, originating from the spherical $i_{13/2}$ state, introduces particularly large Coriolis matrix elements. Since Hjorth, Ryde, and Skånberg were “seeking” a $K^\pi=7^+$ state as the most likely ground state, their artificially small extracted value of K for what turns out to be actually a $K^\pi=9^-$ band led them to interchange the correct positions of their bands.)

Our coincidence results, in agreement with those of Medsker *et al.*, indicate that a rotational band based on a state at 443.1 keV feeds into the 154.1-keV 8^+ member of the $K=7$ band via 289.0-keV interband transition. The assignment of $J^\pi=9^-$ to the 443.1-keV state is based on a number of considerations.

TABLE II. Angular distribution results from the $^{181}\text{Ta}(\alpha,3n\gamma)^{182}\text{Re}$ reaction.

Transition (keV)	Assignment ($J_i \rightarrow J_f$)	K	A_2/A_0	A_4/A_0
154.1	$8^+ \rightarrow 7^+$	7	0.227 ± 0.011	0.037 ± 0.013
185.3	$9^+ \rightarrow 8^+$	7	0.304 ± 0.016	0.044 ± 0.017
212.6	$10^+ \rightarrow 9^+$	7	0.314 ± 0.027	0.045 ± 0.035
237.6	$11^+ \rightarrow 10^+$	7	0.396 ± 0.018	0.072 ± 0.023
260.9	$12^+ \rightarrow 11^+$	7	0.427 ± 0.026	0.081 ± 0.038
282.3	$13^+ \rightarrow 12^+$	7	0.405 ± 0.030	0.081 ± 0.044
339.5	$9^+ \rightarrow 7^+$	7	0.304 ± 0.102	0.058 ± 0.137
397.8	$10^+ \rightarrow 8^+$	7	0.310 ± 0.076	-0.063 ± 0.105
450.1	$11^+ \rightarrow 9^+$	7	0.224 ± 0.029	-0.072 ± 0.035
498.3	$12^+ \rightarrow 10^+$	7	0.335 ± 0.017	-0.135 ± 0.018
543.3	$13^+ \rightarrow 11^+$	7	0.341 ± 0.091	-0.074 ± 0.150
181.8	$10^- \rightarrow 9^-$	9	0.159 ± 0.018	-0.012 ± 0.025
209.3	$11^- \rightarrow 10^-$	9	0.219 ± 0.012	0.032 ± 0.015
234.9	$12^- \rightarrow 11^-$	9	0.261 ± 0.036	0.029 ± 0.049
258.9	$13^- \rightarrow 12^-$	9	0.209 ± 0.058	-0.013 ± 0.075
281.2	$14^- \rightarrow 13^-$	9	0.325 ± 0.151	0.067 ± 0.203
391.2	$11^- \rightarrow 9^-$	9	0.368 ± 0.065	0.002 ± 0.106
444.2	$12^- \rightarrow 10^-$	9	0.451 ± 0.008	0.158 ± 0.012
107.1	$6^- \rightarrow 5^-$	4	-0.382 ± 0.051	0.054 ± 0.091
131.4	$7^- \rightarrow 6^-$	4	-0.384 ± 0.024	0.026 ± 0.036
160.4	$8^- \rightarrow 7^-$	4	-0.469 ± 0.036	-0.021 ± 0.063
217.0	$10^- \rightarrow 9^-$	4	-0.527 ± 0.059	0.142 ± 0.086
95.7	$5^+ \rightarrow 4^+$	2	-0.228 ± 0.031	0.032 ± 0.048
119.5	$6^+ \rightarrow 5^+$	2	-0.266 ± 0.018	0.032 ± 0.028
161.3	$8^+ \rightarrow 7^+$	2	-0.271 ± 0.027	0.065 ± 0.043
289.2	$9^- \rightarrow 8^+$		-0.147 ± 0.006	0.028 ± 0.009
344.6	$15^- \rightarrow 15^-$		0.608 ± 0.119	-0.112 ± 0.159
647.3	$15^- \rightarrow 14^-$		0.591 ± 0.197	0.310 ± 0.317

First, our experimental angular distribution data for the 289.0-keV transition are shown in Fig. 9, where they are superimposed on a plot of a number of calculated angular distributions.²⁵ It can be seen from this figure that the 289.0-keV transition must be either a stretched dipole ($9 \rightarrow 8$) or an $8 \rightarrow 8$ quadrupole. Another argument against the quadrupole transition is that a quadrupole transition from an 8^\pm state would be expected to populate the 7^+ ground state to a much greater extent than the 8^+ 154.1-keV state. (Both the Clebsch-Gordan coefficients and the transition energies favor the 7^+ ground state.) This is not seen experimentally, suggesting a 9^\pm assignment for the 443.1-keV state.

Referring to Fig. 8, we see that the only likely couplings that can produce either $K=8$ or 9 states are the triplet coupling of the $\frac{9}{2}^- [514\uparrow]$ proton with the $\frac{9}{2}^+ [624\uparrow]$ neutron to yield a 9^- state and the singlet coupling of the $\frac{7}{2}^+ [404\downarrow]$ proton with the $\frac{9}{2}^+ [624\uparrow]$ neutron to yield an 8^+ state. The 9^- state is energetically favored to be the 443.1-keV state.

The timing experiments with the 50-ns time scale established that the 154.1- and 289.0-keV γ rays are delayed, coming from a state having a half-life of 6 ± 2 ns. Now,

the single-particle estimates²³ predict half-lives of 1.3×10^{-14} s for a 289.0-keV $E1$ and 1.4×10^{-12} s for an $M1$, yielding retardations of 4.6×10^5 and 4.3×10^3 , respectively. However, $E1$ transitions in deformed nuclei are routinely retarded by such factors (because of violations of selection rules on the asymptotic quantum numbers), whereas corresponding $M1$ transitions are not usually retarded much at all. In fact, although the 289.0-keV transition is probably an $E1$, it involves

$$\pi \frac{9}{2}^- [514\uparrow] \rightarrow \pi \frac{5}{2}^+ [402\uparrow],$$

and its half-life corresponds closely to this observed transition²⁶ in ^{183}Re .

Coincidence relations among the γ transitions enabled us to construct a rotational band on the 443.1-keV state up through the 15^- member. The 281.- and 282.3-keV peaks were not resolved in the integral coincidence spectrum, but, by selectively gating over portions of the composite peak, it was possible to assign them unequivocally to the 9^- and 7^+ bands, respectively. A similar procedure was carried out for the doublets at 303 and 585 keV.

The final argument in favor of the proposed assignment will be considered in more detail in Sec. IV. The intrinsic

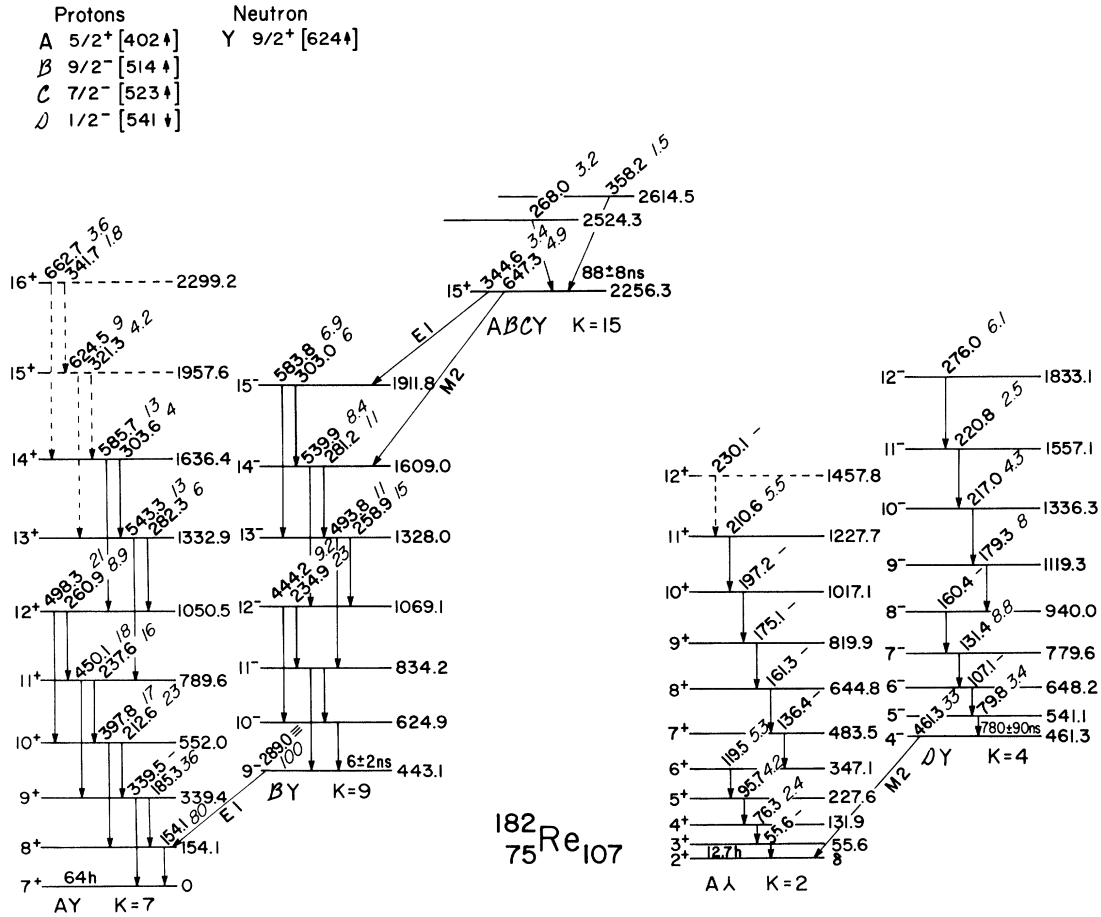


FIG. 6. ^{182}Re level scheme constructed from the present in-beam γ -ray data. All energies are given in keV, and γ -ray intensities (photon intensities not corrected for conversion) are normalized to the 289.0-keV transition. There is no observable isomeric transition between the 2^+ and 7^+ bands. The 7^+ band is presumed to be the ground state (see the text); consequently, energies of states in the 2^+ and 4^- bands are increased by Δ , the separation energy between the 7^+ and 2^+ states. (Assuming these two states to be the triplet and singlet couplings of the same proton-neutron pair, Δ is expected to be of the order of 50 keV.) When the neutron state is inverted (λ), this indicates a singlet coupling. The 15^+ ($ABCY$) configuration is one of two possible for the 2256.3-keV metastable state, the other being 15^- ; see the text for a complete discussion.

gyromagnetic ratio, g_K , obtained for the rotational band built on the 443.1-keV state is inconsistent with an

$$8^+ \{ \pi \frac{7}{2}^+ [404\downarrow] \otimes \nu \frac{9}{2}^+ [624\uparrow] \}$$

assignment but agrees with the

$$9^- \{ \pi \frac{9}{2}^+ [514\uparrow] \otimes \nu \frac{9}{2}^+ [624\uparrow] \}$$

assignment.

B. 2^+ and 4^- bands

Two additional rotational bands were populated intensely enough to allow the characterization of many members in each. These are a low-spin band that meets the requirements for 2^+ $^{182}\text{Re}^m$ as its band head and a medium-spin band based on a state 461.3 keV above $^{182}\text{Re}^m$.

The assignments of the states to the 2^+ band based on $^{182}\text{Re}^m$, the singlet coupling of

$$\pi \frac{5}{2}^+ [402\uparrow] \otimes \nu \frac{9}{2}^+ [624\uparrow],$$

is based on self-consistent, circumstantial evidence. The 55.6-keV $3^+ \rightarrow 2^+$ transition identified in the decay^{1,2} of ^{182}Os could not be found in coincidence gates set on upper members of the band, presumably because of the poor efficiency of the coincidence electronics for low-energy γ rays (cf. below). The 76.3-keV transition was seen clearly only in the spectrum created by summing the coincidence gates set on other members of the band. However, the transition energy, intensity, and angular distribution of this transition are consistent with its assignment to this band—as are those of the other transitions within the band.

No unexplained transitions having energies greater than 70 keV are seen in prompt gates set on the lower spin band members or in the spectrum created by summing delayed gates set to emphasize transitions out of a metastable state. This implies that either the band head has a very long half-life, with the result that no significant number of coincidence events occur within the range of the timing circuit, or that any depopulating transitions have such a low energy that they are either detected with

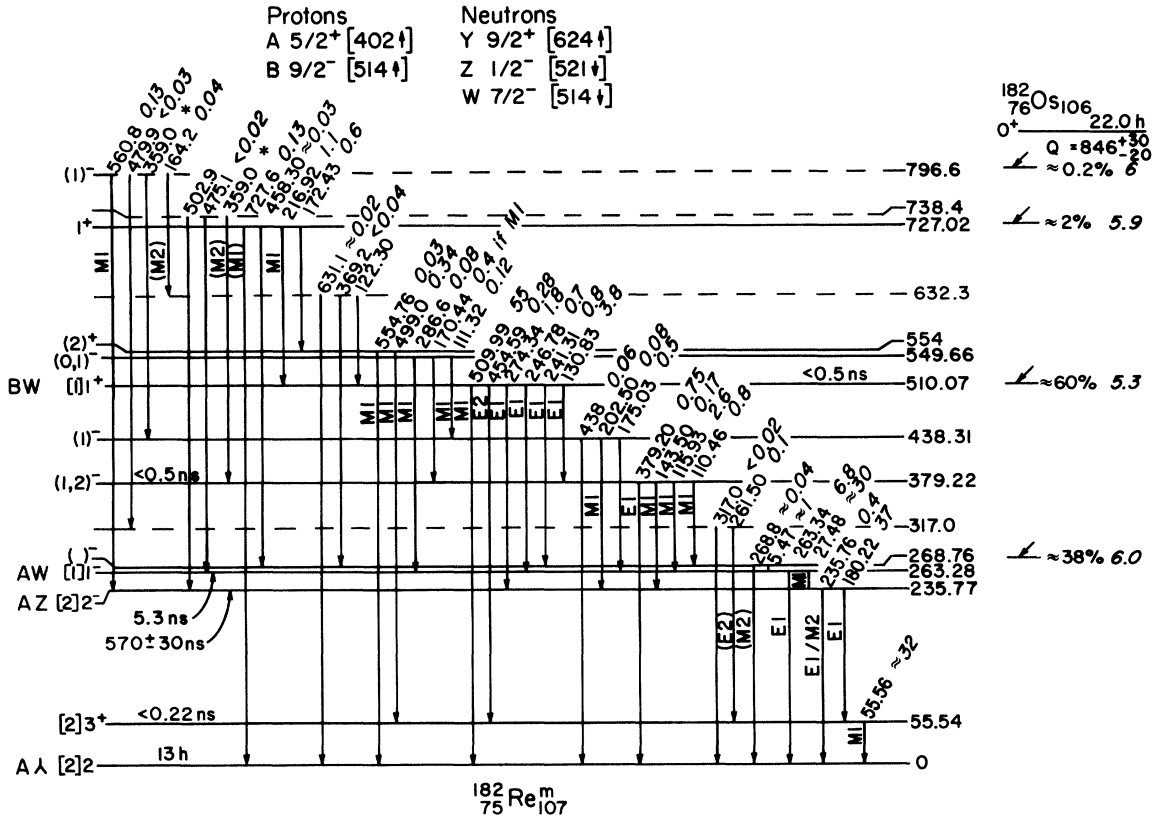


FIG. 7. The decay scheme of ¹⁸²Os. This populates only low-spin states in ¹⁸²Re and is shown for comparison with Fig. 6, which uses the same letters to represent proton and neutron states. This decay scheme is adapted from Refs. 1 and 2; the level placements come from these references, but we have modified some of their state assignments.

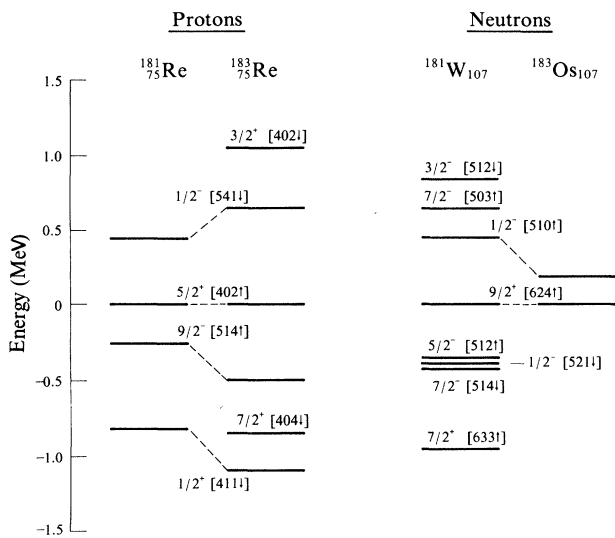


FIG. 8. Experimental single-particle states in neighboring odd-mass nuclei. The A = 181 states were taken from the compilation in Ref. 20; the A = 183 states, from Ref. 21.

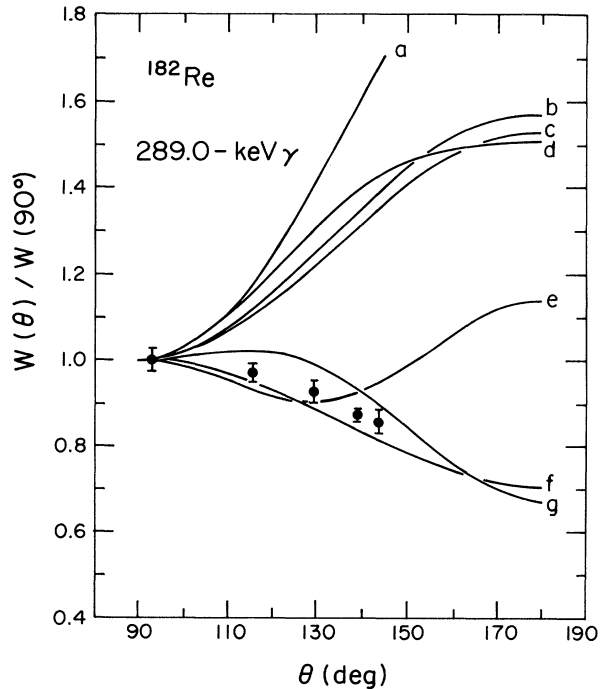


FIG. 9. Angular distributions data points for the 289.0-keV γ transition compared with calculated angular distributions (Ref. 25). The calculated curves correspond to the following $J_i(l)J_f$ values: (a) $J(3)J-3$, (b) $J(3)J-1$, (c) $J(1)J$ or $1(2)1$, (d) $J(2)J-2$, (e) $J(2)J-1$, (f) $J(1)J-1$, and (g) $J(2)J$ except $1(2)1$.

(exceedingly) low efficiency or are masked by x rays. In the latter case, such transitions very likely would feed states that emit at least some γ rays that would be seen in coincidence with transitions within the band. The fact that no such coincident events were observed suggests the former as the more likely possibility. And this, in turn, leads us to suggest that the band head is in fact $^{182}\text{Re}^m$.

The assignment of its members to a 2^+ rotational band having the same moment of inertia as the 7^+ band works out very well within simple empirical band systematics. For example, using the value of $\hbar^2/2\mathcal{I}$ (9.63 keV) found from only the 7^+-8^+ spacing in the 7^+ band yields calculated spins of 1.89, 2.96, 3.97, and 5.21 for the first four members of the 2^+ band. If one accounts for band distortions (cf. Sec. V), the fit is quite good for all the observed members (up to $J^\pi=12^+$), lending further credence to its being the singlet coupling of

$$\pi_{\frac{5}{2}}^+ [402\uparrow] \otimes \nu_{\frac{9}{2}}^+ [624\uparrow].$$

As expected, the transitions within the 2^+ band were seen more intensely relative to transitions in the 7^+ and 9^- bands in the spectra from the (p,n γ) and (p,3n γ) reactions than they were in spectra from the (α ,3n γ) reaction. No predictions of spin based on g factors (cf. Sec. IV) were possible for this band because the angular distributions of transitions within this band are consistent with either positive or negative values of δ .

The band we assigned $K^\pi=4^-$, based on a state 461.3 keV above $^{182}\text{Re}^m$, was populated more strongly by the (α ,3n γ) reaction. Timing data established that the 461.3-keV transition proceeds (directly or indirectly) from a state having a half-life of 780 ± 90 ns. No γ -ray peaks were seen in prompt coincidence gates set on the 461.3-keV peak or in delayed gates set to emphasize transitions fed by the 461.3-keV transitions. From this we conclude that this transition feeds directly either the 7^+ or the 2^+ isomer. Delayed coincidence gates verify that a rotational band is built on the 461.3-keV state: Peaks at 107.1, 131.4, and 160.4 keV were seen directly in the spectra produced by the delayed gates, while transitions between higher members of the band were found from prompt gates set on these three transitions.

The 79.8-keV $5^- \rightarrow 4^-$ transition was not seen in prompt coincidence spectra resulting from gates set on other transitions from the band. This was because of an instrumental problem: the peak of the time-to-amplitude converter (TAC) spectrum became very spread out for γ rays with energies below ≈ 100 keV. The 79.8-keV peak was observed, however, in the spectra resulting from delayed gates set on the 107.1- and 131.4-keV γ rays, and it figured prominently in the spectrum created by summing the delayed gates set on the other intraband transitions. Timing experiments established that the 79.8-keV transition is a "prompt" transition. Further, its energy, intensity, and angular distribution are consistent with its placement in the band.

Deducing the K^π value of this band can be done in two ways, via band systematics and via characteristics of the 461.3-keV transition. Both are consistent with a 4^- assignment.

The transitions associated with this band, including the 461.3-keV depopulating transition, are seen more intensely, relative to transitions associated with the 7^+ and 9^- bands, in the (p,n γ) and (p,3n γ) reactions as opposed to the (α ,3n γ) reaction. This alone suggests that its base spin is somewhat less than 7. Now, deducing spins from band spacings can be somewhat uncertain, since we are dealing with possibly highly distorted bands in this nucleus; there is considerable uncertainty in trying to determine the rotational constant, $\hbar^2/2\mathcal{I}$, *a priori*. Nevertheless, one can make some coarse estimates. Using $\hbar^2/2\mathcal{I}=9.63$ keV, as determined for the 7^+ band, we obtained calculated J values of 3.14, 4.56, 5.82, and 7.33 for the first four members of this new band, using only the $J(J+1)$ term from the rotational energy equation. Using $\hbar^2/2\mathcal{I}=9.09$ keV, as determined for the even more distorted 9^- band, the calculated J values become 3.39, 4.89, 6.23, and 7.82. Note that by this procedure we have (partially) corrected for the tendency of the spins to appear too small because of Coriolis mixing. The 9^- band is more distorted by Coriolis mixing than is the 7^+ band; thus, its $\hbar^2/2\mathcal{I}$ value leads to trial values of spin for the new band that are larger than if we had used the higher values of $\hbar^2/2\mathcal{I}$ as obtained from the 7^+ band. At this point in the deduction process we cannot say whether the unrenormalized $\hbar^2/2\mathcal{I}$ value for this new band is larger or smaller than that for the 9^- band. However, it is clear that there is a large odd-even spacing displacement in this new band, which usually indicates considerable Coriolis mixing. This simple analysis suggests $K=3$ or 4 as possibilities.

TABLE III. ^{182}Re γ -ray half-life estimates.

Single-particle estimates (Ref. 23)		Experiment
461.3-keV transition		
<i>E</i> 1	3.2×10^{-15} s	
<i>M</i> 1	3.5×10^{-13} s	
<i>E</i> 2	6.3×10^{-10} s	
<i>M</i> 2	1.7×10^{-8} s	$7.80 \pm 0.90 \times 10^{-7}$ s
<i>E</i> 3	1.9×10^{-4} s	
<i>M</i> 3	2.5×10^{-3} s	
344.6-keV transition		
<i>E</i> 1	7.6×10^{-15} s	
<i>M</i> 1	8.4×10^{-13} s	
<i>E</i> 2	2.7×10^{-9} s	$\left\{ \begin{array}{l} \text{(see text)} \\ 2.14 \pm 0.20 \times 10^{-7} \text{ s} \end{array} \right.$
<i>M</i> 2	7.6×10^{-8} s	
<i>E</i> 3	1.5×10^{-3} s	
<i>M</i> 3	1.9×10^{-2} s	
647.3-keV transition		
<i>E</i> 1	1.1×10^{-15} s	
<i>M</i> 1	1.2×10^{-13} s	
<i>E</i> 2	1.2×10^{-10} s	
<i>M</i> 2	3.3×10^{-9} s	$1.49 \pm 0.14 \times 10^{-7}$ s
<i>E</i> 3	1.8×10^{-5} s	
<i>M</i> 3	3.9×10^{-4} s	

(The distortions in this and other bands will be considered in greater detail in Sec. V.)

Our measured half-life for the 461.3-keV state, which deexcites solely by the 461.3-keV γ transition, is 780 ± 90 ns. In Table III we show the Weisskopf-Moszkowski single-particle estimates for various multiplicities for this transition. These seem to indicate quite clearly that it is an $M2$ transition. (Even considering that $E1$ transitions in this deformed region are quite often retarded by factors of $\approx 10^6$, an $E1$ does not seem indicated here, and there is no reason *a priori* to suspect severe retardations for the other multiplicities.) The calculated α_K for a 461.3-keV $M2$ is only slightly greater than 0.1, which should not change the single-particle estimate by much. This is quite consistent with the 461.3-keV band head being $J^\pi = 4^-$ and deexciting to the 2^+ $^{182}\text{Re}^m$.

The only low-lying configuration (cf. Fig. 8) for a 4^- band is the triplet coupling of

$$\pi \frac{1}{2}^- [541\downarrow] \otimes \nu \frac{9}{2}^+ [624\uparrow].$$

(The presence of the $\Omega = \frac{1}{2}$ proton state in addition to the $i_{13/2}$ derived $\frac{9}{2}$ neutron state will be shown in Sec. V to account for the extraordinarily severe Coriolis distortion of this band.)

It should be noted that a problem remains concerning the deexcitation pattern of the 4^- 461.3-keV state, viz., the absence of a transition to the 3^+ member of the 2^+ band at 55.6 keV. With our assignments, an $E1$ transition would be highly forbidden, but an $M2$ (or an $E1$ with $M2$ internal selection rules) would be expected. The Clebsch-Gordan factor is 0.31/0.55 for $M2$ branching to the $3^+/2^+$ states. The energy dependence lowers this to 0.30, which makes the absence of such a transition rather surprising. (The Clebsch-Gordan and energy factors strongly discriminate against transitions to the 4^+ or 5^+ members of the 2^+ band.)

The angular distribution of the 461.3-keV γ ray is nearly isotropic (because of the half-life of the 461.3-keV state). However, we did measure a value of $A_2/A_0 = 0.04$, compared with the value of $A_2/A_0 = 0.12 \pm 0.05$ obtained by Hjorth, Ryde, and Skånberg.¹⁷ These results are not conclusive, but they also indicate that the 461.3-keV transition is probably quadrupole. The angular distributions of the intraband transitions establish that δ , the mixing ratio of $E2$ to $M1$ transition amplitudes, is negative. This is also consistent with our assigned configuration, as will be discussed further in Sec. IV.

C. High-lying, high-spin isomer

Data from the "slow" delayed coincidence experiment indicate that all transitions within the 9^- band are delayed. The measured half-life, determined from the decay curves of the 181.8- and 209.3-keV transitions shown in Fig. 10, is 88 ± 8 ns.

Coincidence data revealed that the 15^- and 14^- members of the 9^- band are fed by transitions of 344.6 and 647.3 keV, respectively. A placement of either of these transitions within the band is contrary to predicted rotational behavior. Consequently, these transitions were

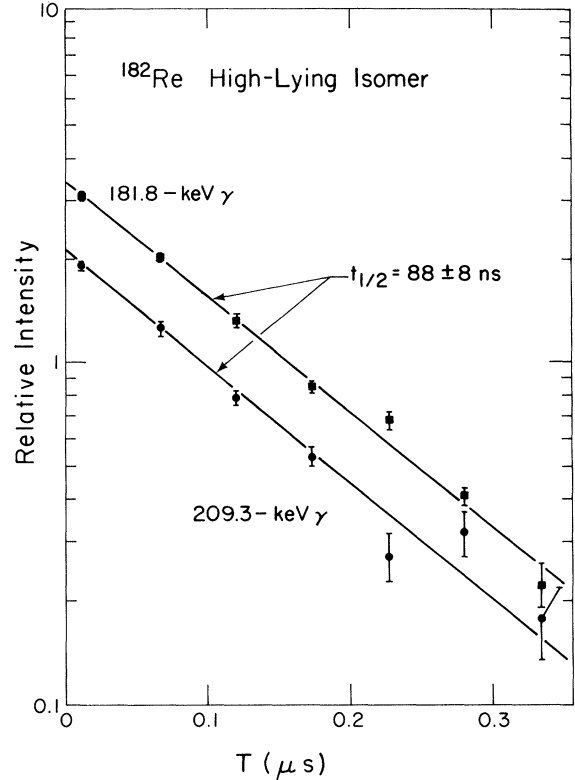


FIG. 10. Half-life determination of the metastable state at 2256.3 keV in ^{182}Re . Decays of two of the more easily fit peaks from transitions in the 9^- rotational band were followed.

placed deexciting a state at 2256.3 keV, having a half-life of 88 ± 8 ns.

Delayed coincidence gates were set on all of the easily resolvable transitions within the 9^- band. The resulting spectra were then summed, and an appropriate fraction of the integral coincidence spectrum was subtracted to eliminate part of the prompt and chance contamination. The resulting spectra are shown in Fig. 11. From these spectra we conclude that transitions of 268.0 and 358.2 keV feed the metastable state at 2256.3 keV. (These two γ rays are not in coincidence with each other.) As a check, delayed gates were set on these peaks to emphasize transitions following the metastable state. In both gates only the 344.6- and 647.3-keV peaks and peaks from transitions within the 9^- band appear. Thus, we conclude that the metastable state decays exclusively through the 9^- rotational band.

The partial half-lives of the 344.6- and 647.3-keV γ transitions are 214 ± 20 and 149 ± 14 ns, respectively. These are compared with single-particle estimates in Table III, where it is seen that they are most compatible with $M2$ assignments. However, since they populate the 15^- and 14^- members of a rotational band, they must necessarily be $E1$ and $M2$ or $M1$ and $E2$, respectively, with or without some compatible admixing. (We can, in this case, safely rule out higher multipolarity combinations on the basis of half-life.) And since $E1$ transitions are notorious-

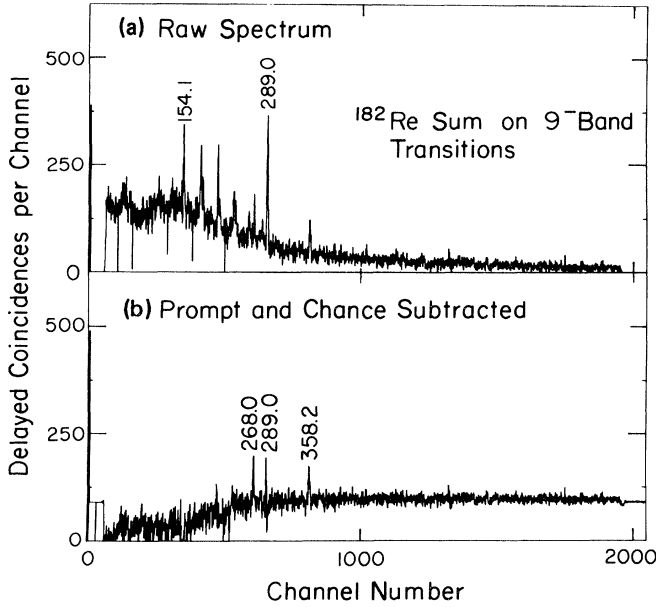


FIG. 11. Delayed coincidence spectrum to show the transitions feeding into the metastable state at 2256.3 keV in ^{182}Re . (a) The sum of delayed gate spectra on all of the easily resolved transitions within the 9^- rotational band. (b) The same spectrum with an appropriate amount of the integral coincidence spectrum (shown in Fig. 2) subtracted to correct partially for prompt and chance contributions.

ly retarded in this region, the $E1$ and $M2$ possibility is the more likely of the two.

The angular distributions of the 344.6- and 647.3-keV γ rays (shown in Fig. 4) are characterized by positive A_2 coefficients. This establishes that neither is a stretched dipole transition. In fact, their angular distributions are quite consistent with the assignment of $J=15$ to the 2256.3-keV metastable state. This would make the 344.6-keV transition a $15 \rightarrow 15$ dipole (+ quadrupole?) and the 647.3-keV transition a $15 \rightarrow 14$ quadrupole.

No hard and fast conclusions can be drawn about the J^π of the 2524.3-keV state from the angular distribution of the 268.0-keV γ ray. This angular distribution only rules out a stretched dipole or a $J \rightarrow J-1$ quadrupole, which indicates that the 2524.3-keV state is not likely a member of a rotational band based on the metastable 2256.3-keV state (unless it were a stretched $E2$, in which case a problem arises concerning a missing $M1$). An angular distribution was not obtained for the 358.2-keV γ ray, but neither is the 2614.5-keV state likely to be a member of such a rotational band, for such a band containing it would have $\hbar^2/2\mathcal{I} = 11.2$ keV, an unreasonable value for this odd-odd nucleus.

Tentative assignment(s) for the principal components of the wave function of the metastable state at 2256.3 keV can be made on the basis of its γ -deexcitation pattern and the available orbits. It should be emphasized that what follows is only a plausibility argument, but its conclusion is consistent with all of the currently available data.

First, the metastable state must be a four-quasiparticle configuration. Its high spin rules out a two-quasiparticle

configuration coupled to a vibrational state, as does its hindered γ deexcitation to the high-spin members of the 9^- rotational band. Second, its deexcitation solely through this 9^- band means its structure must have something in common specifically with this band. Now, all four well-characterized rotational bands contain the uncoupled $\frac{9}{2}^+[624\uparrow]$ neutron state, which means we should focus our attention on the $\frac{9}{2}^-[514\uparrow]$ proton state. To attain a spin as high as 15 means that we need to use the highest spin single-particle orbitals available, viz., these $\frac{9}{2}^+$ orbitals, and recoupling the two $\frac{9}{2}^-[514\uparrow]$ protons to 8^+ , i.e.,

$$\frac{9}{2}^-[514\uparrow] \otimes \frac{7}{2}^-[523\uparrow] = 8^+,$$

is a plausible starting point. Adding the already uncoupled $\frac{9}{2}^-[624\uparrow]$ neutron state to this produces $J^\pi = \frac{25}{2}^+$. To produce the needed spin 15, we need a $\frac{5}{2}^-$ proton state, and the most likely state is $\pi \frac{5}{2}^+[402\uparrow]$. This results in the four-quasiparticle configuration,

$$15^+ \{ \pi \frac{9}{2}^-[514\uparrow] \otimes \nu \frac{7}{2}^-[523\uparrow] \otimes \nu \frac{5}{2}^+[402\uparrow] \otimes \nu \frac{9}{2}^+[624\uparrow] \}.$$

It accounts quite naturally for the positive parity, and it gives the deexciting γ transitions the single-proton character, $\frac{7}{2}^-[523\uparrow] \rightarrow \frac{5}{2}^+[402\uparrow]$, in which one of the uncoupled protons converts to a member of the $J=0$ coupled $\frac{5}{2}^+$ proton pair. The $M2$ transition would be fourfold K forbidden, which accounts nicely for its observed half-life. (The $E1$ would be retarded, as usual, for half a dozen reasons, including fivefold K forbiddenness, not to mention violations of selection rules on asymptotic quantum numbers.) And such a configuration would be expected to deexcite only through the 9^- rotational band.

We can also come up with another plausible configuration,

$$J^\pi = 15^- \{ \pi \frac{9}{2}^-[514\uparrow] \otimes \pi \frac{7}{2}^+[404\downarrow] \otimes \pi \frac{5}{2}^+[402\uparrow] \otimes \nu \frac{9}{2}^+[624\uparrow] \}.$$

The large A_2 values for the 344.6- and 647.3-keV γ rays can suggest highly mixed $\lambda=1$ and 2 transitions, probably $M1/E2$. Here one assumes that n -fold K forbiddenness can be made to account for the relative half-lives. This leads to negative parity for the isomeric state. In addition, as can be discerned from Fig. 8, the $\pi \frac{7}{2}^+[404\downarrow]$ state is expected to lie at a lower energy than the $\pi \frac{7}{2}^-[523\uparrow]$ state.

Thus, both 15^+ and 15^- are possibilities for this four-quasiparticle state. Further studies, using beams of heavy ions to excite and characterize members of the rotational band based on this state should determine which is, in fact, correct.

IV. g FACTORS

The magnitude of the nuclear magnetic moment can be written, apart from a spin factor, as²⁷

$$\mu = (Kg_K + g_R) \frac{J}{J+1}, \quad (1)$$

where g_K and g_R are the intrinsic and rotational gyromagnetic ratios, respectively. For two-quasiparticle states, g_K can be written as

$$Kg_K = \Omega_1 g_{\Omega_1} \pm \Omega_2 g_{\Omega_2}. \quad (2)$$

While g_R is a function of the nuclear shape and is roughly constant (in $^{182}\text{Re} \approx 0.3$) for all rotational bands in a nucleus, g_K is determined by the intrinsic structure of a particular band. Their difference, $g_K - g_R$, is therefore more or less constant over a band and can be related, within the framework of the rotational model, to the mixing ratio, δ^2 :

$$\frac{g_K - g_R^2}{Q_0} = \frac{0.871 E_\gamma^2}{(J+1)(J-1)} \frac{1}{\delta^2}, \quad (3)$$

where Q_0 is the intrinsic quadrupole moment and E_γ is the cascade γ -transition energy in MeV.

The mixing ratio can be determined independent of a specific nuclear model from angular distribution measurements. Using the tables of der Mateosian and Sunyar,²⁸ we evaluated the mixing ratios of some cascade transitions in the 7^+ and 9^- bands. These are given in Table IV. The experimental A_2/A_0 and A_4/A_0 parameters derived from our angular distribution data differ from the theoretical coefficients by the attenuation factors, α_2 and α_4 . These are usually related, under the assumption of a Gaussian magnetic substate population, to the single parameter σ/J , where σ is the standard deviation of the Gaussian distribution and J is the spin of the initial state. The attenuation factors (and hence the value of σ/J) of a state in a rotational band can be determined from the angular distributions of the $E2$ crossover transitions in that same band. σ/J is not expected to vary significantly from state to state, except in the case of metastable states, for

which, of course, the angular distribution of the deexciting transitions can be severely attenuated. Therefore, an average $\sigma/J = 0.32 \pm 0.07$ was used to compute mixing ratios for states in the 7^+ band. This approximation in σ/J is probably responsible for the slight decrease in $|g_K - g_R|/Q_0$ with increasing J , although configuration mixing can have the same result. Adequate angular distributions were not obtained for crossover transitions in the 9^- band, so for this band $\sigma/J = 0.32 \pm 0.07$ was used in the calculation of δ .

In addition, within the framework of the rotational model, the mixing ratio can be calculated from the branching ratio, λ , of crossover to cascade transitions:

$$\frac{1}{\delta^2} = \left[\frac{1}{\lambda} \left(\frac{E_\gamma}{E_{\gamma'}} \right)^5 \frac{(J+1)(J-1+K)(J-1-K)}{2K^2(2J-1)} \right] - 1. \quad (4)$$

Table IV also includes values of δ and $|g_K - g_R|/Q_0$ calculated from experimental branching ratios for the 7^+ and 9^- bands. The transition intensities were taken at 125° with respect to the beam direction. In addition, for transitions in the "delayed" 9^- band, intensities were determined from the "singles" spectrum created by summing the time-band spectra from the "slow" delayed-coincidence experiment. Values of δ and $|g_K - g_R|/Q_0$ derived from these two sets of data were averaged to yield the results listed for the 9^- band.

It can be seen that the mixing ratios calculated by the two methods agree within the experimental uncertainty. Also, the branching-ratio calculations indicate that $|g_K - g_R|/Q_0$ is more or less constant within each band, as predicted by the rotational model. Further, the average

TABLE IV. δ and $|g_K - g_R|/Q_0$ from angular distribution results and branching ratios.

Cascade transition (keV)	J_i	δ_{ad}	δ_{br}	$\frac{ g_K - g_R _{ad}}{Q_0}$	$\frac{ g_K - g_R _{br}}{Q_0}$
154.1	8^+	0.32 ± 0.03		0.056 ± 0.005	
185.3	9^+	0.39 ± 0.05	a	0.050 ± 0.006	
216.6	10^+	0.40 ± 0.06	0.42 ± 0.02	0.050 ± 0.007	0.048 ± 0.002
237.6	11^+	0.49 ± 0.07	0.42 ± 0.02	0.041 ± 0.006	0.048 ± 0.002
260.9	12^+	0.53 ± 0.11	a	0.038 ± 0.008	
282.3	13^+	0.50 ± 0.11	0.41 ± 0.02	0.041 ± 0.009	0.050 ± 0.003
303.6	14^+		0.47 ± 0.06		0.044 ± 0.006
			average	$= 0.046 \pm 0.007$	0.048 ± 0.002
181.8	10^-	0.23 ± 0.02		0.066 ± 0.005	
209.3	11^-	0.32 ± 0.03	0.33 ± 0.02	0.056 ± 0.005	0.055 ± 0.004
234.9	12^-	0.35 ± 0.05	0.34 ± 0.03	0.052 ± 0.007	0.054 ± 0.005
258.9	13^-	0.30 ± 0.07		0.062 ± 0.014	
281.2	14^-	0.42 ± 0.11	0.34 ± 0.02	0.071 ± 0.018	0.056 ± 0.004
303.0	15^-		0.36 ± 0.04		0.053 ± 0.005
			average	$= 0.061 \pm 0.008$	0.055 ± 0.001

*The quadrupole transition needed for the calculation of δ_{br} lies in an unresolved multiplet. Its intensity cannot be determined.

value of $|g_K - g_R|/Q_0$ determined from the angular distribution data agrees with that calculated from the branching-ratio data. We thus have a more or less model independent check for the more precise branching-ratio results.

The intrinsic quadrupole moment, Q_0 , of ^{182}Re has not been measured. However, because Q_0 varies rather slowly over a region, it is possible to use the measured²⁹ Q_0 of ^{182}W , 6.4 b with an assigned uncertainty of 15%. The sign of $g_K - g_R$ is the same as that of δ derived from the angular distribution data. For both the 7^+ and the 9^- bands, δ was found to be positive. Using this value of Q_0 and the average of $|g_K - g_R|/Q_0$ from the branching-ratio calculations, we obtain, for the 7^+ band,

$$g_K - g_R = 0.29 \pm 0.05. \quad (5)$$

The g factor of 64-h $^{182}\text{Re}^g$ has been measured³⁰ to be 0.399 ± 0.008 . This can be substituted into Eq. (1) for the magnetic moment. Assuming $K=7$ for the ground-state band, Eqs. (1) and (5) can be solved simultaneously for g_K and g_R , yielding $g_K = 0.44 \pm 0.02$ and $g_R = 0.15 \pm 0.07$. This value for g_R is significantly smaller than the expected 0.3, although values this small have been found³¹ in ^{161}Dy and ^{177}Hf .

g_K can be determined independently from Eq. (2) and the empirical values of g_Ω from the neighboring odd-mass nuclei for the $\frac{5}{2}^+[402\uparrow]$ proton and the $\frac{9}{2}^+[624\uparrow]$ neutron.³² This yields $g_K = 0.43$, in agreement with our experimental result.

One possible explanation for the unusually small value obtained for g_R is that Q_0 of ^{182}Re is really much smaller than the values used from neighboring nuclei. It is clear, however, that either g_R or Q_0 deviates substantially from the anticipated value.

The small value of g_R for ^{182}Re obtained here might be expected on the basis of partially confirmed calculations of g_R for several nearly odd-mass nuclei performed by Prior, Boehm, and Nilsson.³³ They predicted that ^{179}Hf and ^{181}W have g_R values of 0.14 (or 0.12) and 0.05, respec-

tively. This reduction in g_R , as compared to that of other odd-mass nuclei, was attributed to the influence of the outer-shell nucleons, in particular the $\frac{9}{2}^+[624\uparrow]$ neutron, which, of course, is also at work in ^{182}Re . In an odd-odd nucleus,

$$\mathcal{J} = \mathcal{J}_p + \mathcal{J}_n. \quad (6)$$

Also,

$$g_R = \frac{\mathcal{J}_p}{\mathcal{J}} = \frac{\mathcal{J}_p}{\mathcal{J}_p + \mathcal{J}_n}. \quad (7)$$

Generally, both \mathcal{J}_p and \mathcal{J}_n for an odd-odd nucleus will be greater than the corresponding values for a nucleus comprised of one fewer proton or one fewer neutron. However, by comparing the values of $\hbar^2/2\mathcal{J}$ for ^{182}W , ^{181}Re , and ^{182}Re (estimated from the energy difference of the first two states of the ground-state rotational bands), one finds that, while the odd proton of ^{182}Re does little to increase \mathcal{J}_p over that of ^{181}W , its odd neutron dramatically increases \mathcal{J}_n over that of ^{181}Re . Thus, one might expect the g_R of ^{182}Re to be smaller than the g_R of ^{181}Re and close to g_R of ^{181}W . The predictions of Prior, Boehm, and Nilsson for ^{181}W have not been tested experimentally. However, their similar predictions for ^{167}Er and ^{161}Dy have been confirmed.

Table V lists values of g_K calculated in the asymptotic limit of the deformation parameters compared with the experimental values of g_K obtained from branching ratios in the 7^+ and 9^- bands. Q_0 was assumed to be 6.4 b, and g_R was taken to be 0.15. Although the calculations were carried out in the asymptotic limit of deformation, no significant changes are introduced when Nilsson wave functions for a deformation appropriate to ^{182}Re are used.³⁴ It can be seen that the experimental value of g_K is quite consistent with the

$$9^- \{ \pi \frac{9}{2}^- [514\uparrow] \otimes \nu \frac{9}{2}^+ [624\uparrow] \}$$

assignment.

TABLE V. Calculated versus experimental values of g_K .

Proton	Neutron	K	Calculated ^a g_K	Experimental ^b g_K (7^+ band)	Experimental ^b g_K (9^- band)
$\frac{5}{2}^+[402\uparrow]$	$\frac{9}{2}^+[624\uparrow]$	7	0.39	0.44	0.63
$\frac{5}{2}^+[402\uparrow]$	$\frac{7}{2}^- [514\downarrow]$	6	0.96	0.50	0.74
$\frac{9}{2}^- [514\uparrow]$	$\frac{9}{2}^+[624\uparrow]$	9	0.52	0.37	0.50
$\frac{7}{2}^+[404\downarrow]$	$\frac{9}{2}^+[624\uparrow]$	8	0.03	0.39	0.55
$\frac{5}{2}^+[402\uparrow]$	$\frac{5}{2}^- [512\uparrow]$	5	1.15	0.60	0.88
$\frac{5}{2}^+[402\uparrow]$	$\frac{7}{2}^+[633\uparrow]$	6	0.42	0.50	0.74

^aCalculated from the asymptotic expression,

$$g_K = 1/K \{ (g_{sn}\Sigma_n + g_{in}\Lambda_n) \pm (g_{sp}\Sigma_p + g_{ip}\Lambda_p) \}.$$

^bCalculated from γ -ray branching ratios according to Eqs. (3) and (4), assuming $Q_0 = 6.4$, $g_R = 0.15$, and $V_{g_s, \text{eff}} = 0.8g_{s, \text{free}}$.

If the validity of the rotational model is assumed and g_R and Q_0 are known, then g_K can be determined from the experimental mixing ratio, δ . This experimental g_K can be compared with calculated predictions, thereby serving as an aid in identifying the components of states in the band structure. Unfortunately, branching ratios were not obtained for our proposed (and rather more weakly populated) 2^+ and 4^- bands, and the angular distribution results for transitions within these bands were insufficient to allow us to determine δ . However, the angular distributions of the cascade transitions in the proposed 4^- band did establish that the sign of δ , and hence of $(g_K - g_R)$, is negative. This means that $g_K < g_R$, a requirement that limits the possible assignments for the band head. In Table VI we list calculated values for a variety of states possibly expected at rather low excitation in ^{182}Re . Of these, only three $K = 1$, the $K = 4$ and 5 states from the

$$\pi \frac{1}{2}^- [541\downarrow] \otimes \nu \frac{9}{2}^+ [624\uparrow]$$

TABLE VI. Predicted values of g_K for possible bands in ^{182}Re .

Proton	Neutron	K (triplet) (singlet)	Calculated ^a g_K
$\frac{5}{2}^+ [402\uparrow]$	$\frac{9}{2}^+ [624\uparrow]$	7	0.39
		2	-2.88
$\frac{5}{2}^+ [402\uparrow]$	$\frac{7}{2}^- [514\downarrow]$	1	-5.76
		6	0.96
$\frac{9}{2}^- [514\uparrow]$	$\frac{9}{2}^+ [624\uparrow]$	9	0.52
		0	
$\frac{7}{2}^+ [404\downarrow]$	$\frac{9}{2}^+ [624\uparrow]$	1	-3.29
		8	0.03
$\frac{1}{2}^- [541\downarrow]$	$\frac{9}{2}^+ [624\uparrow]$	4	0.07
		5	-0.55
$\frac{5}{2}^+ [402\uparrow]$	$\frac{1}{2}^- [510\uparrow]$	3	0.90
		2	2.88
$\frac{5}{2}^+ [402\uparrow]$	$\frac{5}{2}^- [512\uparrow]$	5	1.15
		0	
$\frac{5}{2}^+ [402\uparrow]$	$\frac{1}{2}^- [521\downarrow]$	2	1.35
		3	1.92
$\frac{5}{2}^+ [402\uparrow]$	$\frac{7}{2}^+ [633\downarrow]$	6	0.45
		1	-5.77

^aFrom the asymptotic expression (with $g_{s,\text{eff}} = 0.8g_{s,\text{free}}$),

$$g_K = 1/K \{g_{sp}\Sigma_p + g_{lp}\Lambda_p\} \pm (g_{sn}\Sigma_n + g_{ln}\Lambda_n) \} .$$

configuration and the $K = 8$ state from the singlet coupling of

$$\pi \frac{7}{2}^- [404\downarrow] \otimes \nu \frac{9}{2}^+ [624\uparrow] ,$$

are consistent with $g_K \leq 0.3$. For reasons already discussed in Sec. III B, it is unlikely that the 780 ± 90 ns 461.3-keV state has spin as high as 8 or as low as 1. Further, the triplet coupling is expected to lie lower in energy than the singlet. Thus, we have here a corroboration of our assigning the

$$4^- \{ \pi \frac{1}{2}^- [541\downarrow] \otimes \nu \frac{9}{2}^+ [624\uparrow] \}$$

configuration as the principal component of the 461.3-keV band head.

V. BAND PARAMETERS AND BAND DISTORTIONS

In Fig. 12 the rotational spacings of the four lower-lying, most completely characterized bands are plotted in the conventional manner to emphasize distortions in these spacings. Such a plot is designed to produce a straight line for a rotational band that follows the equation,

$$E = E_0 + AJ(J+1) + BJ^2(J+1)^2 . \quad (8)$$

A is usually comprised primarily of $\hbar^2/2\mathcal{I}$, although the Coriolis effect can often introduce a negative contribution, which lowers A from the value found for nearby even-even and, to a lesser extent, from the value for neighboring odd-mass nuclei. B is small and negative for even-even nuclei and is usually associated with "centrifugal stretching." For other than even-even nuclei, Coriolis effects can often add larger, positive components to the B term. (This combination of a negative contribution to A and a positive contribution to B is why bands distorted by Coriolis effects can appear to have a spin smaller than their actual spin.)

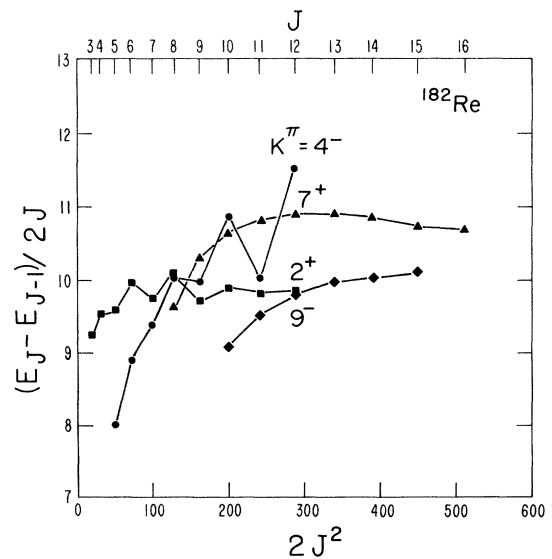


FIG. 12. Rotational spacings of lower-lying bands in ^{182}Re , showing the anomalous spacings, particularly in the $K^\pi = 2^+$ and 4^- bands.

From the spacing in Fig. 12 it is obvious that the band distortions are severe and require more to explain them than a straightforward application of the Coriolis force up through the $J^2(J+1)^2$ term. In particular, the 4^- and 2^+ bands show odd-even distortions characteristic of $K = \frac{1}{2}$ bands, of $K=0$ admixtures, or of bands that are beginning to decouple from the rotational core.³⁵⁻³⁷ A complete odd-odd Coriolis calculation, however, is beyond the scope of the present paper and will be deferred to a later publication.

A further question arises with respect to the possibility of backbending in odd-odd nuclei and in this nucleus in particular. Although with the $(\alpha, 3n\gamma)$ reaction we have not really reached the requisite rotational angular momentum for backbending in a corresponding even-even system, it is instructive to consider the situation.

In Fig. 13 we show a conventional "backbending" graph, in which the moment of inertia,

$$2\mathcal{I}/\hbar^2 = (4R' - 2)/(E_j - E_{j-2}),$$

with $R' = J - j$, is plotted against the square of the rotational frequency

$$[\hbar^2\omega^2 \approx 1/4(E_j - E_{j-2})^2].$$

This type of plot removes the odd-even effects, provided the "favored" and "unfavored" levels show the same sort of behavior within their half-bands, and it can be seen that the curves of Fig. 13 are indeed rather smoothly varying ones (with the possibility of some residual distortion in that for the 4^- band). Also, there is no evidence for backbending, at least up to these only moderately large rotational levels.

This is only negative evidence, but it does add a bit more to the argument that backbending is primarily a result of rotational alignment³⁸ of high- Ω particles rather than the breaking down of pairing.³⁹ This has already been demonstrated rather conclusively for odd-mass nuclei, where, presuming that the breaking and rotation aligning of an $i_{13/2}$ neutron pair was the major factor in even-even backbending, it was found that odd-neutron nuclei did not backbend,⁴⁰ whereas odd-proton nuclei did.³⁷ In other words, the odd neutron was already occupying the $\alpha = \frac{13}{2}$ (α , the projection along the rotation axis) state, making the breaking and aligning of an $i_{13/2}$ pair less favorable energetically, whereas the odd proton had no such effect.

Now, in this odd-odd nucleus there are both an odd neutron and an odd proton to block the advantages of

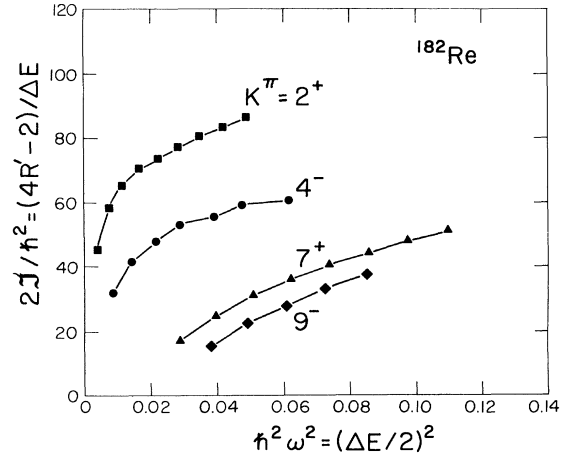


FIG. 13. Behavior of the rotational bands in ^{182}Re shown on a conventional "backbending" type of plot, i.e., a plot designed to emphasize changes in the moment of inertia such as associated with backbending.

breaking and aligning particles. Thus, whether it is the $i_{13/2}$ neutron pair or the $h_{9/2}$ proton pair that contributes most strongly to even-even backbending in this region does not matter; for either case backbending is less energetically favorable for an odd-odd nucleus than for an even-even nucleus until considerably higher spins are reached.

Another question that arises from the graphs in Fig. 13 is the magnitude of the moments of inertia. Clearly, the simple analysis of such a plot does not adequately account for the spread in the curves. This is most obvious for the 7^+ vs 2^+ bands, which are primarily triplet and singlet couplings of the same

$$\pi \frac{5}{2}^+ [402\uparrow] \otimes \nu \frac{9}{2}^+ [624\uparrow]$$

configuration.

VI. FOUR-QUASIPARTICLE ISOMER

We were able to characterize the metastable state at 2256.3 keV in ^{182}Re as a $K^\pi = 15^+$ or 15^- state (cf. Sec. III C) and, from its deexcitation pattern, to infer that the most important component of its wave function is the four-quasiparticle configuration,

$$15^+ \left\{ \pi \frac{9}{2}^- [514\uparrow] \otimes \left\{ \begin{array}{l} \pi \frac{7}{2}^- [523\uparrow] \\ \pi \frac{7}{2}^+ [404\downarrow] \end{array} \right\} \otimes \pi \frac{5}{2}^+ [402\uparrow] \otimes \nu \frac{9}{2}^+ [624\uparrow] \right\}.$$

A moot point arises concerning the role of this state's structure in the competition for angular momentum degrees of freedom at high spins.

The possible competition between collective and few-

nucleon degrees of freedom in carrying large amounts of angular momentum has been discussed by Diamond and Stephens⁴¹ and by Bohr and Mottelson.⁴² Also, four- and six-quasiparticle high-spin "yrast and near-yrast traps"

have been identified in even-even Hf nuclei.^{43,44} We conclude that the $K=15$ state in ^{182}Re is such a few-quasiparticle state and that it may very well begin to add an “oblate” contribution in the form of a girdle about the basically prolate shape.

Classically, an oblate spheroid rotating *about* its symmetry axis (oblate-||) has the largest moment of inertia [$\mathcal{I} \approx \mathcal{I}_0(1+0.6\beta)$, where β is the usual deformation parameter, slightly larger than $\Delta R/R$] and consequently produces the lowest lying rotational states.⁴¹ This oblate-|| is followed in energy by a prolate spheroid rotating about an axis perpendicular to its symmetry axis (prolate- \perp), which has $\mathcal{I} \approx \mathcal{I}_0(1+0.3\beta)$, then by oblate- \perp [$\mathcal{I} \approx \mathcal{I}_0(1+0.3\beta)$] and prolate-|| [$\mathcal{I} \approx \mathcal{I}_0(1+0.6\beta)$]. In a quantum-mechanical system such as nuclei, of course, the rotations about the axes of symmetry are not defined and the corresponding collective rotations do not exist. However, Bohr and Mottelson⁴² pointed out that it ought to be possible to have *effective* rotational states about such axes consisting of few-nucleon states, i.e., the coupled few-neutron orbitals can “effectively” act as members of a “rotational” band, each member being a *different* few-nucleon state. By such a mechanism an *effective* oblate-|| rotational band could become yrast or nearly yrast at excitations where multiquasiparticle states are energetically possible.

In Fig. 14 we show in a very stylized way how such a four-quasiparticle configuration as the $K=15$ metastable state could begin to make an “effective oblate” contribution to the rotation. In this figure the orbits and quantum numbers could refer to any four nucleons, although the lengths have been adjusted to fit $\Omega_1 = \frac{5}{2}$, $\Omega_2 = \frac{7}{2}$, $\Omega_3 = \frac{9}{2}$, and $\Omega_4 = \frac{11}{2}$, so that they could be the three protons and one neutron of the $K=15$ state. The $\pi_{\frac{5}{2}}^+[402\uparrow]$ state originates from the $d_{5/2}$ spherical orbit, so it is the highest- Ω deformed state associated with that orbit and has its \vec{j} most aligned along the axis of symmetry. (Of course, \vec{j} is not strictly a good quantum number in these deformed systems, and for each Ω one gets a mixture of \vec{j} 's from the various spherical states. Nevertheless, for small values of β the largest single \vec{j} contribution comes from the spherical \vec{j} state from which the deformed state

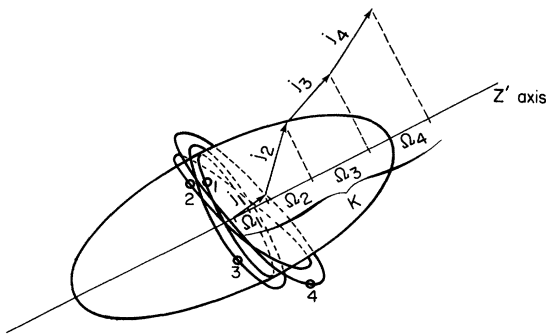


FIG. 14. Stylized sketch showing four high- Ω quasiparticles with their angular momenta uncoupled and aligned along the symmetry axis. These four nucleons provide an “effective” oblate girdle about a basically prolate core.

originated. This is particularly true for the high-spin, opposite parity spin-orbit-toward intruder states such as $i_{1/32}$ and $h_{11/2}$, but it remains valid enough not to affect the qualitative arguments in this section.) The $\pi_{\frac{9}{2}}^- [514\uparrow]$ and $\pi_{\frac{7}{2}}^- [523\uparrow]$ states originate from the spherical $h_{11/2}$ state, and the $\nu_{\frac{9}{2}}^- [624\uparrow]$ from the $i_{13/2}$; thus, these are not aligned maximally along the symmetry axis, but their alignment is largely in that direction. (The $\pi_{\frac{7}{2}}^+ [404\downarrow]$ state for the alternate 15^- configuration from the $g_{7/2}$ state also is aligned basically in that direction.) The four quasiparticles contribute a focus of sorts around the midriff of the prolate core. This focus will contribute an “oblate-||” quantity toward the moment of inertia; hence, this type of structure could well lie lower than some collective prolate- \perp rotational states. *The entire nucleus has not become oblate*, however, for the Fermi surface lies in the wrong place to favor high- Ω oblate Nilsson states. With either of the two (15^+ or 15^-) configurations, this state is an example of a strong-coupled high- K isomer, corresponding here still to a prolate- \perp configuration, but using single-particle degrees of freedom to carry much of the angular momentum.

According to this picture, the state,

$$16^+ \{ \pi_{\frac{11}{2}}^- [505\uparrow] \otimes \pi_{\frac{7}{2}}^- [523\uparrow] \\ \otimes \pi_{\frac{5}{2}}^+ [402\uparrow] \otimes \nu_{\frac{9}{2}}^+ [624\uparrow] \},$$

and particularly the most aligned state,

$$17^+ \{ \pi_{\frac{11}{2}}^- [505\uparrow] \otimes \pi_{\frac{9}{2}}^- [514\uparrow] \\ \otimes \pi_{\frac{5}{2}}^+ [402\uparrow] \otimes \nu_{\frac{9}{2}}^+ [624\uparrow] \},$$

should lie nearby at higher energies. (The $\pi_{\frac{11}{2}}^- [505\uparrow]$ state lies only slightly further from the Fermi surface than does the $\pi_{\frac{7}{2}}^- [523\uparrow]$ state.) Obviously, we do not have enough information to identify either of these. With heavy-ion beams to excite states of higher spin, tracing the prolate versus oblate and single particle versus core competitions should make a fascinating field of investigation.

VII. CONCLUSIONS

Relatively little in-beam γ -ray spectroscopy has been performed on odd-odd nuclei, partly because it has been assumed the resulting spectra would be so complicated that the difficulty of analysis would not be worth the effort. For ^{182}Re this has turned out not to be true, for the myriad of deexciting rivulets have all more or less converged into only four rivers flowing into four rotational bands. Very likely this will also be true for other deformed odd-odd nuclei, making their study a profitable field.

Heavier ions than α particles are needed, however, to explore the regions of high rotational angular momentum. For example, although we reached states with spin as high as 16 in these ($\alpha, 3n\gamma$) studies, we excited states only as high as 10 units of rotational angular momentum. The remainder went into the high-spin intrinsic degrees of freedom, which, of course, are interesting in their own right.

Aside from the straightforward spectroscopy of odd-odd states, this work has demonstrated three fields of pursuit more or less unique to deformed odd-odd nuclei:

(1) *Exploration of the Coriolis effect.* Bands in odd-odd nuclei can become extremely distorted because of Coriolis perturbations. The Coriolis operators are single-particle operators, and odd-odd nuclei provide twice as many particles and a far greater density of states with which to work, especially at low excitation energies. Also, the singlet and triplet states can be coupled together through higher order terms because the doubling over of the $K = \frac{1}{2}$ state connects singlet and triplet odd-odd states. Many of the singlet and triplet states will lie quite close together, allowing a favorable exploration of higher order Coriolis couplings.

(2) *Yrast and near-yrast traps.* Odd-odd nuclei are ideal microlaboratories for finding and elucidating such states. Here, especially, more work needs to be done at higher rotational angular momentum. Experiments using beams of heavier ions are needed. A thorough examination of the oblate versus prolate, few particle versus collective competition ought to yield some rather fundamental information about nuclear makeup.

(3) *Backbending and perturbations in band structure caused by large rotational angular momenta.* Although the rotationally aligned explanation of backbending seems rather firmly established, this work on odd-odd ^{182}Re has added some slight evidence against the pairing-collapse

explanation of backbending. Examination of higher rotational states, both in this and in other odd-odd deformed nuclei, would be a straightforward way in which to explore this further.

In summary, we have shown in this paper that in-beam γ -ray studies of odd-odd nuclei, although complex, are quite tractable. With today's high-resolution, multiscanner, computer-monitored experiments, they should be a prime field of interest, especially at accelerators producing beams of very heavy ions.

ACKNOWLEDGMENTS

Many people have contributed their aid unselfishly to aid us with this paper. In particular, we wish to thank Dr. W. Bentley, Dr. R. B. Firestone, and Dr. P. Walker for their help with the data taking and analysis. We also sincerely thank Dr. F. S. Stephens, Dr. R. M. Diamond, Dr. J. O. Rasmussen, and Dr. J. M. Diriki for helpful and enlightening discussion concerning the interpretations. One of us (W.C.M.) also thanks Dr. J. O. Rasmussen and the Nuclear Science Division of LBL for their hospitality during his sabbatical leave there, where this work was completed. This material is based on work supported by the U.S. National Science Foundation under Grant No. PHY 78-01684 and by the U.S. Department of Energy under Contract DE-AC03-76SF0098.

*Present address: Harvard Law School, Cambridge, MA 02138.

†Present address: Battelle Pacific Northwest Laboratories, Richland, WA 99352.

‡Present address: Physics Division, Argonne National Laboratory, Argonne, IL 60439.

§Present address: Office of the Dean, College of Sciences and Humanities, Iowa State University, Ames, IA 50011.

¹S. B. Burson, P. J. Daly, P. F. A. Goudsmit, and A. A. C. Klasse, Nucl. Phys. **A204**, 337 (1973).

²B. Svahn, C. Bergman, A. Johansson, B. Nyman, W. Dietrich, and N. Ibrahiem, Phys. Scr. **7**, 257 (1973).

³A. I. Akhmadzhanov, R. Broda, V. Valyus, I. Zvol'ski, I. Molnar, Ya. Stychen', V. I. Fominykh, A. Khrynkevich, and V. M. Tsupko-Sitnikov, Izv. Akad. Nauk SSSR, Ser. Fiz. **34**, 777 (1970).

⁴W. Andrejtscheff, L. Funke, W. Meiling, and F. Sary, Nucl. Phys. **A135**, 170 (1969).

⁵Z. Plajner, V. Brabec, and L. Maly, Czech. J. Phys. **19B**, 1616 (1969).

⁶B. Harmatz and T. H. Handley, Nucl. Phys. **A121**, 481 (1968).

⁷J. O. Newton, Phys. Rev. **117**, 1510 (1960).

⁸R. Spanhoff, M. J. Canty, H. Postma, and G. Mennenga, Phys. Rev. C **21**, 361 (1980).

⁹B. D. Jeltema, F. M. Bernthal, T. L. Khoo, and C. L. Dors, Nucl. Phys. **A280**, 21 (1977).

¹⁰P. Galan and M. Vejs, Czech. J. Phys. **22B**, 18 (1972).

¹¹J. J. Sapyta, E. G. Funk, and J. W. Mihelich, Nucl. Phys. **A139**, 161 (1970).

¹²V. I. Gavriyuk, V. T. Kupryashkin, G. D. Latyshev, I. N. Lyutyi, Y. V. Makovitskii, and A. I. Feoktistov, Izv. Akad. Nauk SSSR, Ser. Fiz. **35**, 2232 (1971).

¹³P. Galan, T. Galanova, Z. Malek, N. Voinova, Z. Preibisz, and K. Stryczniewicz, Nucl. Phys. **A136**, 673 (1969).

¹⁴B. Harmatz, T. H. Handley, and J. W. Mihelich, Phys. Rev. **123**, 1758 (1961).

¹⁵C. J. Gallagher, Jr., and V. G. Soloviev, K. Dan. Vidensk. Selsk. Mat.-Fys. Skr. **2**, No. 2 (1962).

¹⁶C. J. Gallagher and S. A. Moszkowski, Phys. Rev. **111**, 1282 (1958).

¹⁷S. A. Hjorth, H. Ryde, and B. Skånberg, Ark. Fys. **38**, 537 (1968).

¹⁸L. R. Medsker, G. T. Emery, P. P. Singh, L. A. Beach, and C. R. Gossett, Bull. Am. Phys. Soc. **16**, 515 (1971).

¹⁹J. T. Routti and S. G. Prussin, Nucl. Instrum. Methods **72**, 125 (1969).

²⁰Y. A. Ellis, Nucl. Data Sheets **2**, 319 (1973).

²¹A. Artna-Cohen, Nucl. Data Sheets **16**, 267 (1975).

²²H. Rubinsztein and M. Gustafsson, Phys. Lett. **58B**, 283 (1975).

²³S. A. Moszkowski, in *Alpha-, Beta- and Gamma-Ray Spectroscopy*, edited by K. Siegbahn (North-Holland, Amsterdam, 1965), Chap. XV.

²⁴A. K. Kerman, K. Dan. Vidensk. Selsk. Mat.-Fys. Medd. **30**, No. 15 (1956).

²⁵D. G. McCauley, unpublished calculations.

²⁶P. P. Singh, L. R. Medsker, G. T. Emery, L. A. Beach, and L.

- R. Gossett, *Phys. Rev. C* **10**, 656 (1974).
- ²⁷P. Alexander, F. Boehm, and E. Kapkeheit, *Phys. Rev.* **133**, B284 (1969).
- ²⁸E. der Mateosian and A. W. Sunyar, *At. Data Nucl. Data Tables* **13**, 391 (1974); **13**, 407 (1974).
- ²⁹K. E. G. Lobner, M. Vetter, and V. Honig, *Nucl. Data* **A7**, 495 (1970).
- ³⁰E. Hagn, P. Kienle, and G. Eska, in *Proceedings of International Conference on Hyperfine Interactions Studied in Nuclear Reaction and Decay, Uppsala, Sweden, 1974*, edited by E. Karlsson and R. Wäppling (Upplands Grafiska AB, Uppsala, 1974), p. 122.
- ³¹C. Hubel, C. Gunther, K. Krien, H. Toschinski, K. H. Speidel, B. Klemme, G. Kumbartzki, L. Gidefeldt, and E. Bodenstecht, *Nucl. Phys.* **A127**, 609 (1969).
- ³²T. L. Khoo, Ph.D. thesis, McMaster University, 1974, p. 67 (unpublished).
- ³³O. Prior, F. Boehm, and S. G. Nilsson, *Nucl. Phys.* **A110**, 257 (1968).
- ³⁴S. G. Nilsson, *Dan. Vidensk. Selsk. Mat.-Fys. Medd.* **29**, No. 16 (1955).
- ³⁵F. S. Stephens, *Rev. Mod. Phys.* **47**, 43 (1975).
- ³⁶F. S. Stephens, R. M. Diamond, and S. G. Nilsson, *Phys. Lett.* **44B**, 429 (1973).
- ³⁷E. Grosse, F. S. Stephens, and R. M. Diamond, *Phys. Rev. Lett.* **32**, 74 (1974).
- ³⁸F. S. Stephens and R. Simon, *Nucl. Phys.* **A183**, 257 (1972).
- ³⁹B. R. Mottelson and J. G. Valatin, *Phys. Rev. Lett.* **5**, 511 (1960).
- ⁴⁰E. Grosse, F. S. Stephens, and R. M. Diamond, *Phys. Rev. Lett.* **31**, 840 (1973).
- ⁴¹R. M. Diamond and F. S. Stephens, *Annu. Rev. Nucl. Part. Sci.* **30**, 85 (1980).
- ⁴²A. Bohr and B. R. Mottelson, *Nuclear Structure* (Benjamin, Reading, Mass., 1975), Vol. II, pp. 43ff, 72ff.
- ⁴³T. L. Khoo, F. M. Bernthal, R. G. H. Robertson, and R. A. Warner, *Phys. Rev. Lett.* **37**, 823 (1976).
- ⁴⁴T. L. Khoo and G. Løvholden, *Phys. Lett.* **67B**, 271 (1977).